PHOTOSYNTHETICA
International Journal for Photosynthesis Research

DOI 10.32615/ps.2023.043 PHOTOSYNTHETICA 61 (SI): 483-491, 2023

Special issue in honor of Prof. Győző Garab

Microdomains heterogeneity in the thylakoid membrane proteins visualized by super-resolution microscopy

R. KAŇA*,+, B. ŠEDIVÁ*,**, and O. PRÁŠIL*

*Centre Algatech, Institute of Microbiology of the Czech Academy of Sciences, Opatovický mlýn, 379 81 Třeboň, Czech Republic**
*Faculty of Science, University of South Bohemia in České Budějovice, Branišovská 31a, 370 05 České Budějovice, Czech Republic***

Abstract

The investigation of spatial heterogeneity within the thylakoid membrane (TM) proteins has gained increasing attention in photosynthetic research. The recent advances in live-cell imaging have allowed the identification of heterogeneous organisation of photosystems in small cyanobacterial cells. These sub-micrometre TM regions, termed microdomains in cyanobacteria, exhibit functional similarities with granal (Photosystem II dominant) and stromal (Photosystem I dominant) regions observed in TM of higher plants. This study delves into microdomain heterogeneity using super-resolution Airyscan-based microscopy enhancing resolution to approximately ~125 nm in x-y dimension. The new data reveal membrane areas rich in Photosystem I within the inner TM rings. Moreover, we identified analogous dynamics in the mobility of Photosystem II and phycobilisomes; countering earlier models that postulated differing mobility of these complexes. These novel findings thus hold significance for our understanding of photosynthesis regulation, particularly during state transitions.

Keywords: Airyscan; cyanobacteria; FRAP; microdomain; photosystem; protein mobility; super-resolution microscopy; thylakoid membrane heterogeneity.

Introduction

Spatial heterogeneity in thylakoid proteins (Mullineaux and Liu 2020) and lipids (Austin *et al.* 2006, Garab *et al.* 2017) is vital for efficient photosynthesis. Thylakoid membranes (TMs) house diverse protein complexes that capture light energy, converting it into high ATP/ADP and NADPH/NADP$^+$ ratios *via* light-driven electron and proton transports. Key players in the process include Photosystem I (PSI) and Photosystem II (PSII) complexes, which collaborate with light-harvesting proteins, like phycobilisomes or TM-embedded proteins from the LHC

Highlights

- A heterogeneous mosaic of photosystems is visible as microdomains in cyanobacteria
- Super-resolution microscopy reveals Photosystem I-enriched inner membrane layers
- Comparable mobility of Photosystem II and phycobilisomes in cyanobacterial thylakoids

Received 3 November 2023
Accepted 1 December 2023
Published online 18 December 2023

+Corresponding author
e-mail: kana@alga.cz

Abbreviations: Chl – chlorophyll; Cyt b_6f – cytochrome b_6f complex; NDH – NADH dehydrogenase complex; PBS – phycobilisomes; PPCs – pigment–protein complexes namely Photosystem I, Photosystem II, and phycobilisomes; TM – thylakoid membrane; YFP – yellow fluorescence protein.

Acknowledgements: The work on this long-term project was supported by the GACR project 23-06593S, by the ERC project Photoredesign (No. 854126), and by institutional project Algatech (MSMT LO1416) and Algamic provided by the Czech Ministry of Education, Youth and Sport (CZ.1.05/2.1.00/19.0392). The authors want to thank our previous confocal technicians and post-docs (Dr. G. Konert and Dr. E. Semanat) for their valuable experimental and practical inputs given during the period of Airyscan detector adaptation in our laboratory. Finally, we also express our gratitude for the inspiration that have emerged throughout the project solution.
Conflict of interest: The authors declare that they have no conflict of interest.

family (Kirilovsky and Büchel 2019). These pigment–protein complexes form supercomplexes, observable *in vitro* through advanced techniques such as electron and atomic force microscopy (Dekker and Boekema 2005, Zhang *et al.* 2021). Remarkably, similar protein organization occurs in living cells, as thylakoid membrane microdomains or nanodomains (Casella *et al.* 2017, Strašková *et al.* 2019, Abram *et al.* 2022). The functional role of these microdomains, primarily comprised of pigment–protein complexes (PPCs), is emerging as a new focal point in photosynthetic research, given the predominant presence of pigmented proteins among TM proteins (Jackson *et al.* 2023). Microscale heterogeneity in thylakoids is evident in the granal/stromal architecture of plant thylakoids (Mustárdy and Garab 2003, Pribil *et al.* 2014). This diversity was initially spotted using electron microscopy [*see* the historical review in Austin and Staehelin (2011)] and later linked to PSI and PSII separation in plant chloroplasts (Andersson and Anderson 1980, Anderson 1981). Debate persisted over whether this separation also existed in organisms without this unique membrane architecture, such as red algae, diatoms, dinoflagellates (Solymosi 2012) or cyanobacteria (Mareš *et al.* 2019). The original idea was that only higher plants and green algae showed PSI/PSII heterogeneity, while cyanobacteria lacked it (Mullineaux 2005, Wilhelm *et al.* 2020). However, later research revealed PSI/PSII heterogeneity even in single-celled algae (Lepetit *et al.* 2012, Flori *et al*. 2017), and in cyanobacteria (Vermaas *et al.* 2008, Steinbach *et al.* 2015, Casella *et al.* 2017, Strašková *et al.* 2019). Cyanobacteria exhibited grana/stroma-like heterogeneity in the lateral PSI/PSII localization without visible membrane stacking. The heterogeneity was named photosynthetic microdomains (Strašková *et al.* 2019). It seems that the heterogeneity in the distribution of photosystems plays a pivotal role in the overall efficiency of photosynthesis in all oxygenic phototrophs. It impacts various aspects of photosynthesis [*see e.g.*, Gu *et al.* (2022)], including minimizing energy spillover between photosystems, regulating ATP/NADPH ratios (Anderson *et al.* 1995), and affecting processes of photoprotection and protein repair (Herbstová *et al.* 2012, Rast *et al.* 2019).

New live-cell imaging techniques [*see e.g.*, the review on cyanobacteria by Yokoo *et al.* (2015)] can reveal how changes in the distribution of proteins within cells relate to their role in photosynthesis. Several *in vivo* microscopic methods have already advanced our understanding of cyanobacteria (Vermaas *et al.* 2008, Casella *et al.* 2017, MacGregor-Chatwin *et al.* 2017, Strašková *et al.* 2019, Canonico *et al.* 2021, Crepin *et al.* 2021, 2022; Huokko *et al.* 2021, Kaňa *et al.* 2021). These methods, while valuable, have a limitation – they generally provide lower spatial resolution compared to more popular techniques such as cryo-electron microscopy (Engel *et al.* 2015, Rast *et al.* 2019, Weiner *et al.* 2022) or atomic force microscopy (Casella *et al.* 2017, MacGregor-Chatwin *et al.* 2017, Zhao *et al.* 2022). Recent improvements in confocal microscopy methods have boosted their sensitivity. They have enabled the discovery of photosynthetic microdomains due to PSI/PSII heterogeneity in single-celled cyanobacteria (Steinbach *et al.* 2015, Konert *et al.* 2019, Strašková *et al.* 2019), identified a spotty localization of respiratory complexes in cyanobacterial thylakoids [*e.g.*, NDH – Liu *et al.* (2012)], and heterogeneity in ATPase and cytochrome b_6f, and other auxiliary TM proteins such as FtsH proteases, Vipp protein or CurT protein (Heinz *et al.* 2016, Gutu *et al.* 2018, Krynická *et al.* 2023). Additionally, special microscopic techniques have revealed heterogeneity in fluorescence lifetimes that reflect the efficiency of photosynthesis (Bhatti *et al.* 2021, Verhoeven *et al.* 2023) or different protein mobility (Casella *et al.* 2017, Kaňa *et al.* 2021).

Despite the progress, there remain several unanswered questions in photosynthetic research because of the limited resolution of *in vivo* methods. In our current study, we show details in the mosaic of TM microdomains in native cyanobacteria cells thanks to the application of the new technology, a hexagonally packed detector array of Airyscan (Huff 2015). The increased resolution allowed us to show a high abundance of PSI-rich membrane areas inside the inner TM rings. Additionally, the time-lapse super-resolution imaging has indicated that PBS and PSII mobility does not seem to be significantly different in their *in vivo* trafficking in contrast to some previous results obtained by other less-native methods for the detection of protein trafficking in TM.

Materials and methods

Cell culture: We used the glucose-tolerant (GT), a non-motile variant of strain *Synechocystis* sp. PCC6803, coming from the laboratory of Prof. Peter Nixon at Imperial College London (Tichý *et al.* 2016). The used GT sub-strain evolved from the motile sub-version of the *Synechocystis* sp. strain originally allocated in the *Pasteur Culture Collection 6803 – Synechocystis* sp. PCC 6803 (Williams 1988). GT variant used in this study represents the main model version of PCC 6803 used in many laboratories as it represents the closest variant of the originally motile *Pasteur Culture Collection 6803* strain (Tichý *et al.* 2016). Its ability to grow on glucose allows its heterotrophic cultivation that was not applied in our study. In our case, we cultivate the GT strain autotrophically and the variant with fluorescently tagged PSI (Strašková *et al.* 2018, 2019), hereafter called *Synechocystis PSI-YFP*, was used. Cells were cultivated autotrophically, on an orbital shaker (T = 28°C) in BG11 medium at continuous light [35 μmol(photon) m^{-2} s^{-1} was provided by warm-white LEDs]. All experiments were carried out with cells in the exponential growth phase (OD_{730} = 0.2–0.3 measured with *WPA S800* Diode Array Spectrophotometer, *Biochrom Ltd*., England). The minimal effect of YFP tagging at PSI on cell physiology, and protein composition has been already proved (Strašková *et al.* 2019, Canonico *et al.* 2021).

Standard and super-resolution laser scanning confocal microscopy: Cells for confocal imaging were prepared and images were acquired by a method slightly modified

from our previous papers (Strašková *et al.* 2019, Konert *et al.* 2019, Canonico *et al.* 2021). The experiments were carried out with our Laser Scanning Confocal Microscope (*Zeiss LSM 880*, *Carl Zeiss Microscopy GmbH*, Germany) equipped with a Plan–Apochromatic 63×/1.4 Oil *DIC M27* objective. The standard confocal and Airyscan images were taken subsequently on the same cells, with the same pixel size (0.053 µm), the same laser excitation and very similar detection ranges for YFP, Chl, and phycobilisome emission.

The standard confocal microscopy setup was following: (*1*) YFP fluorescence from PSI was excited by argon laser 488 nm (laser power 0.7%), fluorescence emission was captured by GaAsP-detector (gallium arsenide phosphide) at wavelengths 526–588 nm (gain 900, MBS 488, pinhole set to 53 µm); (*2*) Chl autofluorescence from PSII was excited by argon laser 488 nm (laser power 0.7%), and signal was detected at 695–758 nm by PMT (photomultiplier) detector (gain 900, MBS 488, pinhole set to 53 µm); (*3*) PBS were excited by helium–neon laser at 594 nm (laser power 0.07%) and PBS fluorescence was detected by GaAsP emission range 642–677 nm (gain 805, pinhole 63 µm, MBS 488/594). Pixel dwell time was 33.0 µs for all the channels.

The super-resolution was acquired by the Airyscan detector that represents a hexagonally packed grid of 32 GaAsP sub-detectors used for image deconvolution (Huff 2015). We used the following setup: (*1*) YFP fluorescence from PSI was excited by argon laser 488 nm (laser power 1% from maximal laser power of 2.1 mW) and fluorescence emission was detected at wavelengths 526–555 nm (gain 900, MBS 488/594, pinhole set to 161 µm); (*2*) Chl fluorescence from PSII was excited by argon laser 488 nm (0.7% from maximal laser power 2.1 mW) and captured by LP filter 685 nm (gain 800, MBS 488/594, pinhole set to 161 µm); (*3*) PBS fluorescence was excited by helium–neon laser at 594 nm (0.07% from maximal laser power 0.75 mW) and captured by BP filter (655–685 nm, gain 800, MBS 488/594, pinhole set to 161 µm). The pixel dwell time was 8.2 µs for all three channels. The Airyscan images were processed by *ZEN Black* software (Huff 2015).

Results and discussion

We successfully identified photosynthetic microdomains within the native *Synechocystis* sp. PCC 6803 strain using fluorescently tagged PSI-YFP *Synechocystis PSI-YFP*, as depicted in the confocal images presented in Fig. 1. Consistent with previous findings (Strašková *et al.* 2019), our analysis revealed two distinct main regions: (*1*) the PSI-dominant area, marked by a green colour (*see e.g.*, green star in Fig. 1*A* and 1*C*); and (*2*) the PSII and PBS-dominant region characterized by a lower PSI signal, identified by a magenta colour (*see e.g.*, magenta star in Fig. 1*A* and 1*D*), resembling grana-like structures [*see* for instance Strašková *et al.* (2019)]. These regions mirrored the functional equivalent of partial spatial separation observed in photosystems (PSI and PSII) in the thylakoid membranes of higher plants, known as grana (dominated by PSII) and stroma (dominated by PSI). Hence, in this context, the green microdomain within cyanobacterial thylakoids is referred to as ‘stroma-like’ thylakoids due to its higher PSI content, while the magenta region is designated as ‘grana-like’ thylakoids due to its higher PSII content.

We stepped further in the spatial resolution and explored these microdomains with an Airyscan detector (*see* comparison in Fig. 2). The detector allows amplification of spatial resolution of the standard detector up to about 120 nm in x-y axes and amplifies also the signal to noise ratio [*see* for instance its description in Huff (2015)]. We consequently imaged the identical cells by standard confocal detector and then the Airyscan detector. The images showed the presence of two main microdomains during image acquisition by Airyscan detection; there were both, grana (*see* magenta in Fig. 2) and stroma-like (*see* green area in Fig. 2) membrane regions in thylakoids. In addition, compared to the previous data with the standard confocal detector, the Airyscan detector was

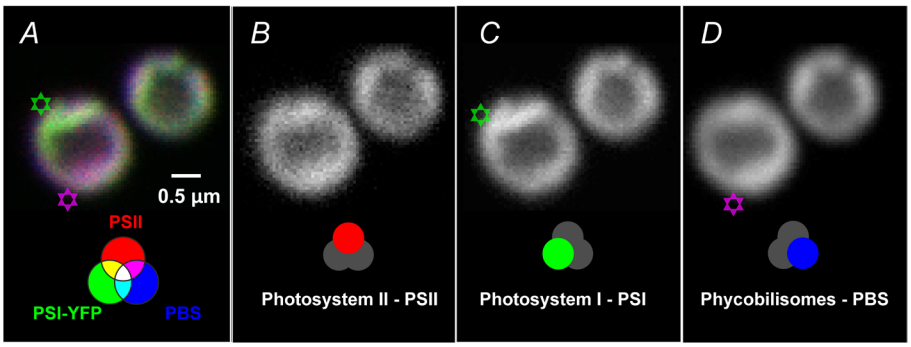

Fig. 1. Typical 3-channel visualization of photosynthetic microdomains in *Synechocystis* sp. PCC 6803 *PSI-YFP* cells acquired by standard confocal method [*see e.g.*, Strašková *et al.* (2019) for method description]. (*A*) RGB picture (red-green-blue) combined from three detected channels of chlorophyll emission from PSII (red channel), YFP fluorescence from PSI (green channel), and phycobilisome emission (blue channel). Panels (*B*), (*C*), and (*D*) then represent single channels pictures used for RGB picture. *The magenta/green stars* represent an example of two main microdomains types: grana-like – magenta area with dominant PSII and PBS signal (less YFP-PSI emission); stroma-like – green areas with dominant PSI and less PBS and PSII signal.

able to visualize some specific TM areas (*see* orange and yellow arrows in Fig. 2*A* and 2*C*). It includes some small and thin 'PSI-rich rings' of TM regions (*see* orange arrow in Fig. 2*A*) or partial separation of outer/inner membranes layer with higher/lower signal of PSI-YFP (*see* orange in Fig. 2*C*). This is in line with the previous suggestion that PSI-rich areas more often dominate the inner membrane layers and PBS + PSII signal was dominant rather in the outer layers [*see* Vermaas *et al.* (2008)]. Even though the separation of the inner/outer TM rings is on the border of the spatial resolution of our instrument (Huff 2015) it is higher than the previously used hyperspectral confocal instrument (Vermaas *et al.* 2008). Therefore, we suggest that PBS and PSII are indeed more dominant in the outer layers of thylakoids.

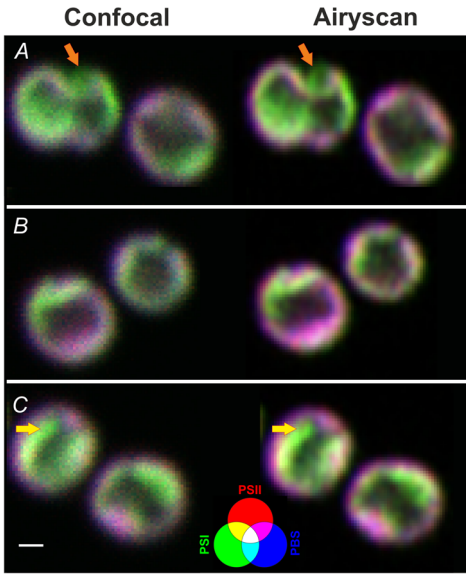

Fig. 2. Direct comparison of the same *Synechocystis* sp. PCC 6803 *PSI-YFP* cells were imaged by the standard confocal detector or by the Airyscan detector. Panels (*A*), (*B*), and (*C*) represent selected cells from the whole set of images (*see* data in Fig. 1S). The pictures represent RGB (red-green-blue) images combined from three detected channels of chlorophyll emission from PSII (Photosystem II) – red channel, YFP fluorescence from PSI (Photosystem I) – green channel, and PBS (phycobilisomes) emission – blue channel (*see* additive color bar scheme in panel *C*). Magenta then represents a combination of PSII (red) and PBS (blue) with minimal contribution of green (PSI). Scale bar 0.5 µm.

The radial heterogeneity in the localization of the three main pigment–protein complexes (PPCs) has been further explored by detailed image analysis (Fig. 3). The analyses allowed us to identify their co-localization across thylakoid membrane layer in two typical cells (Fig. 3*B*,*C*): The 'cell no. 1' clearly showed higher fluorescence signal of YFP from PSI in the inner membrane layers (*see* the shift in the maximum of the green channel intensity in comparison to blue and red in Fig. 3*B*); the remaining two proteins (PSII – red channel; phycobilisomes – blue channel) were more intensively co-localized at the outer membrane layers (*see* the shift in their maximum in Fig. 3*B*). However, this was not typical for all cells, for instance in 'cell no. 2' (Fig. 3*C*) the signal of PSI-YFP was more often co-localised with PSII (red) then in 'cell no. 1' (Fig. 3*B*). It shows that the higher abundance of PSI in the inner layer is not present in all cells (*see* Fig. 1S, *supplement*), because of the cell-to-cell heterogeneity, known for the microbial population in general (Gasperotti *et al.* 2020), and indeed, we typically detected so for the *Synechocystis PSI-YFP* cells (Canonico *et al.* 2020). However, we have almost never detected cells where PSII and/or PBS were more abundant in the inner layers

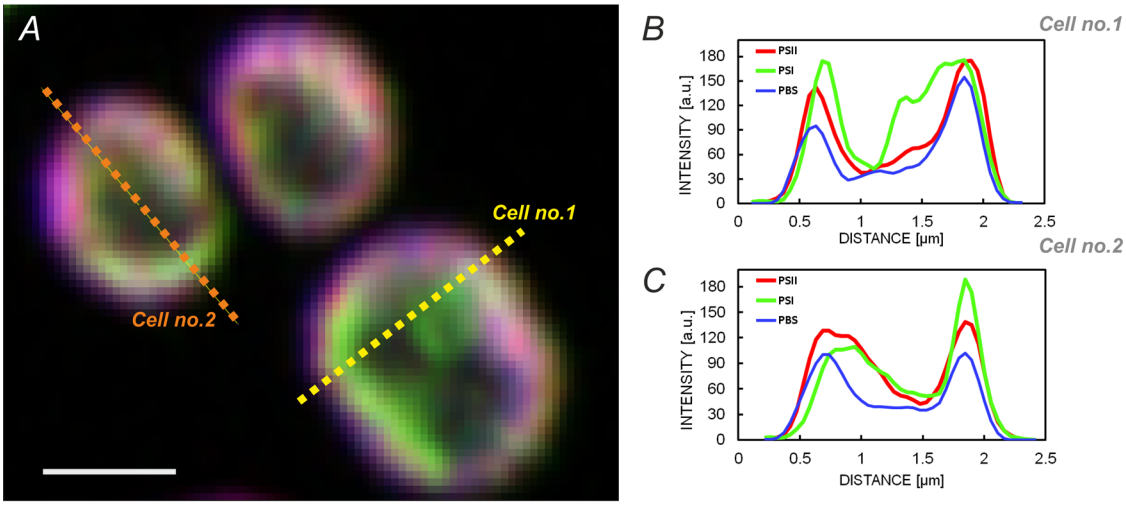

Fig. 3. The typical radial co-localization of Photosystem I, Photosystem II, and phycobilisomes in *Synechocystis* sp. PCC 6803 with *PSI-YFP* detected by the Airyscan detector. (*A*) The pictures represent RGB (red-green-blue) images combined from three detected channels of chlorophyll emission from PSII (red channel), YFP fluorescence from PSI (green), and phycobilisome emission (blue) as described in the Fig. 1. Panels (*B*) and (*C*) represent spatial profiles in the fluorescence intensities in the free channels across the cell no. 1 (*B*) and cell no. 2 (*C*). The colours represent the fluorescence intensities of acquired channels, Photosystem II (red), YFP from Photosystem I (green), and phycobilisomes (blue). Scale bar 1 µm.

of thylakoids (*see* Fig. 1S). It shows that there is some prerequisite why PSI complex is more often localised in the inner membrane sheets of thylakoids. The functional importance of the effect requires additional research with specific mutants. However, we are prone to suggest that the inner membrane layers rich in PSI represent areas of thylakoids more suitable for membrane complex assembly or protein synthesis (Mahbub *et al.* 2020) that, however, contrast with other cyanobacterial species like *Synechococcus* sp. PCC 7942 (Huokko *et al.* 2021).

The application of Airyscan also made it possible to study fluorescence kinetics inside single cells (Fig. 4) and on subcellular compartments (Fig. 5). The measurements were allowed by the significantly improved signal-to-noise ratio of the acquired image (*see* Fig. 2). The dynamic changes in Chl and phycobilisomes autofluorescence during the time-lapse imaging were analysed (*see* Fig. 4). The applied scanning laser (488 nm for Chl emission from PSII; 632 nm for phycobilins emission from PBS) acted as photo-activation source of light that caused variable autofluorescence induction typical for phototrophs. The analysed kinetic data from single cells showed that continuous irradiation of single cells resulted in the fluorescence increase in the case of PBS (Fig. 4*B*) and a decrease in the Chl emission from PSII (Fig. 4*B*) for blue light excitation. This is in line with the bulk measurements with cell suspension where PBS fluorescence in the PBS-containing cyanobacteria

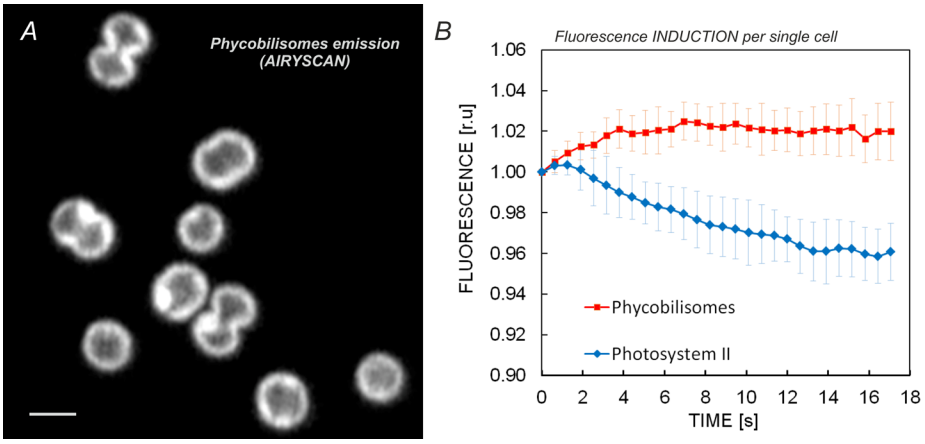

Fig. 4. Photosynthetic fluorescence induction kinetics detected from the single cells of *Synechocystis* sp. PCC 6803 by the Airyscan detector. The data were obtained by time-lapse imaging of cyanobacterial cells (time step of 632 ms) in their autofluorescence of PSII (chlorophyll emission: excitation 488 nm, 14.7 µW per focal area, detection range – LP 685 nm) and PBS (phycobilisomes emission: excitation 633 nm, 0.525 µW per focal area, detection range 650–685 nm). (*A*) Typical PBS images. (*B*) Kinetics of fluorescence intensities of PBS and Photosystem II from the single cell during time-lapse imaging. Data represent averages of several cells (n = 18) from two independent measurements. Scale bar 2 µm.

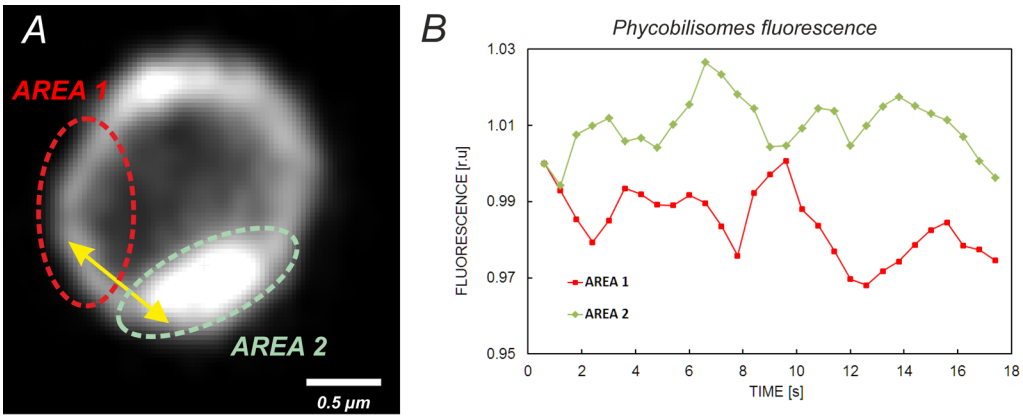

Fig. 5. Time and spatial fluorescence fluctuation in the phycobilisomes signal inside of thylakoid membrane areas of *Synechocystis* sp. PCC 6803. Phycobilisomes (PBS) fluorescence from thylakoids was detected every 0.60 seconds by the Airyscan detector (pixel size ~ 33 × 33 nm, excitation: 633 nm, detection range: 650–680 nm). (*A*) Approximate positions of the selected thylakoid membrane areas – Area 1 and Area 2. *The yellow arrows* indicate the proposed directions of PBS trafficking in 2D approximation. (*B*) Calculated fluorescence intensity of PBS fluorescence is visible as intensity fluctuations in the thylakoid membrane compartments (Area 1 and 2, *see* Fig. 3S). Data represent averaged behaviour of fluorescence signal in the selected membrane areas of one cell. For the online version of the movie, *see* the enclosed Movie 1S or the online link https://youtu.be/KTCJZSyA1E0?si=nR-WUvvCzV9zvi6Y.

increases after orange irradiation (Kaňa *et al.* 2009, 2012) and the Chl fluorescence is quenched after blue light irradiation. In the bulk measurements, the blue light-induced decrease has been attributed to the OCP-dependent quenching (Wilson *et al.* 2006) that indicating its importance also for the Chl fluorescence decrease on the single-cell level (Fig. 4*B*). The slow fluorescence rise was then attributed to state transitions (Kaňa *et al.* 2012). To confirm that the interpretation is also valid for our single cells' measurements, the microscopic experiments with the selected mutants (ΔOCP and ΔApcD) need to be done in future experiments.

The kinetic data on single-cell level have shown that Chl and PBS fluorescence induction acquired by Airyscan represents a useful method to study fluorescence changes on a single-cell level similarly as it has been described by Komárek *et al.* (2010). We stepped even further and analysed acquired time-lapsed images on the sub-cellular level of microdomains (*see* sub-cellular TM compartments visible in green/magenta in the Fig. 1, 2, and 3). We analysed kinetic fluorescence changes in PBS (Fig. 5) and Chl (*i.e.*, PSII) fluorescence (Fig. 3S, *supplement*) in the two neighbouring membrane compartments – Area 1 and Area 2. The data showed more complex behaviour of these small areas. The comparison of their fluorescence fluctuations indicated a functional correlation between these two specific areas – the increase in Area 1 was often (although not every time) accompanied by a decrease in the PBS fluorescence inside the neighbouring Area 2 (Fig. 5). This is a typical sign of the spatial-temporal correlation in the fluorescence signal, a sign of proteins trafficking between these two areas. The spatial or temporal correlation is often used as a method for detection of the fast diffusion events inside of single native cells – the method is called Fluorescence Correlations Spectroscopy [*see e.g.*, results for cyanobacteria (Kaňa *et al.* 2021) or for chloroplasts (Iwai *et al.* 2013) for temporal correlations or Raster Image Correlation Spectroscopy method for spatial/temporal correlations (Malacrida *et al.* 2018)]. We have not run detailed numerical analyses, however, even the rough calculations have already indicated the presence of fluctuations in the PBS signal between two areas (Fig. 5) – it is a sign/indication of PBS trafficking on the TM surface. Similarly, the same result was obtained for Chl emission from PSII (Fig. 3S). The data need more detailed analyses and control experiments with mutants to get numerical values of diffusion with the 100-nm scale spatial resolution. However, even the first analyses showed that the mobility measured by a steady-state correlation method indicated a similar diffusion rate of PBS and PSII (compare the fluctuation pattern in Fig. 5 and Fig. 3S; the movement was also visible in the movies, *see* Movies 1S and 2S, *supplement*). This is in contrast to some older data rather based on a non-steady state method for diffusion measurements – Fluorescence Recovery After Photobleaching (FRAP), for reviews *see e.g.*, Kaňa (2013), Kirchhoff (2014), Mullineaux (2008). The original results with cyanobacteria claimed that PBS are mobile elements on the TM surface in contrast to rather immobile PSII (Mullineaux *et al.* 1997). It seems that these conclusion needs to be re-evaluated as FRAP is rather non-steady state method that requires perturbation of the system by the short bleach (Mueller *et al.* 2010, Lippincott-Schwartz *et al.* 2018). In the specific case of photosynthetic proteins [for the most recent reviews *see e.g.*, Kaňa (2013), Kirchhoff (2014), Mullineaux (2008)] FRAP measurements with PBS can become a complicated task *in vivo* [*see e.g.*, Liu *et al.* (2008)] as PBS photo-physics during FRAP bleaching is sensitive to some specific artefacts [*see e.g.*, discussion in Muzzopappa and Kirilovsky (2020)]. For instance, it is known that PBS excitation is connected with reversible fluorescence blinking (Gwizdala *et al.* 2018) that can affect the interpretation of fluorescence recovery during FRAP methods [*see e.g.*, discussion on GFP blinking in Mueller *et al.* (2012)]. Therefore, our new experimental system applying time-lapse super-resolution imaging (*see* Fig. 5, Fig. 2S, Movie 1S and 2S) represents a promising *in vivo* method to solve whether there is a significant difference in photosystems and PBS mobility [*see e.g.*, the first results by FRAP obtained almost 25 years ago – Mullineaux *et al.* (1997)]. Our first super-resolution time-lapse imaging data show (especially the enclosed movies Movie 1S and 2S, and Fig. 5, Fig. 3S) that PBS and PSII mobility are not significantly different as proposed previously based on FRAP (Mullineaux *et al.* 1997). To quantify rather small differences in PSII and PBS mobility, a new methodology of image analysis needs to be implemented for future experiments (Scipioni *et al.* 2018) with mutants deficient in the regulation of photosynthesis connected with PBS mobility [*e.g.*, during state transitions, *see* Joshua and Mullineaux (2004)].

In conclusion, the application of the Airyscan detector for *in vivo* imaging of thylakoid membrane proteins (especially PSI, PSII, and PBS) proved its high applicability for the cyanobacterial system of TM. Therefore, the method seems to be promising for super-resolution imaging of larger TM system proteins in plant/algal chloroplasts. The method can thus help to solve several open questions; for example, whether the PBS mobility is significantly higher in comparison to PSII or how the TM protein mosaic operates in light of rather limited diffusion of proteins in thylakoids that is 100–1,000 times slower in comparison to the mitochondrion [*see e.g.*, the review of Kaňa (2013), Kirchhoff (2014), Mullineaux (2008)]. Moreover, a forthcoming comparative study that integrates super-resolution microscopy with AFM/EM will offer a comprehensive understanding of protein organization dynamics within TM in terms of proteins stability and dynamics. Recent AFM/EM data obtained from isolated thylakoids suggest the presence of stable protein arrays of TM proteins [*see*, for instance, MacGregor-Chatwin *et al.* (2017)]. However, this finding seems to contradict the continuous protein trafficking observed *in vivo* using super-resolution methods (*see* supplementary Movies 1S and 2S; Iwai *et al.* 2014). There is a big hope that application of the newly emerging super-resolution methods such as the Airyscan (Fig. 2), SpiRI (Single Pixel Reconstruction Imaging; Chenebault *et al.* 2020), SIM (MacGregor-Chatwin *et al.* 2017, Iwai

et al. 2018, Hepworth *et al.* 2021, Flannery *et al.* 2023), SCLIM (Iwai *et al.* 2016) or expansion microscopy (Wassie *et al.* 2019) could shed a light on all these open questions. Our data showed the applicability of one specific super-resolution method – Airyscan, for the small phototrophic cells of cyanobacteria. Altogether, all the new super-resolution methods mentioned above represent an improvement in two directions: (*1*) they have a sub-diffraction resolution in comparison to standard LS confocal methods; (*2*) they can study dynamic protein behaviours in living cells within the grana/stroma-like membrane compartments (*e.g.*, in microdomains/nanodomains, Strašková *et al.* 2019). In this sense, they overcome the major drawbacks of EM and AFM methods – the necessity of TM isolation that does not allow to study behaviours of dynamic proteins in thylakoids (Iwai *et al.* 2014, MacGregor-Chatwin *et al.* 2017). Moreover, the super-solution Airyscan method is suitable for detecting proteins trafficking in thylakoid membrane compartments as it is visible in our results.

References

Anderson J.M.: Consequences of spatial separation of photosystem 1 and photosystem 2 in thylakoid membranes of higher plant chloroplasts. – FEBS Lett. **124**: 1-10, 1981.

Anderson J.M., Chow W.S., Park Y.-I.: The grand design of photosynthesis: Acclimation of the photosynthetic apparatus to environmental cues. – Photosynth. Res. **46**: 129-139, 1995.

Andersson B., Anderson J.M.: Lateral heterogeneity in the distribution of chlorophyll-protein complexes of the thylakoid membranes of spinach chloroplasts. – BBA-Bioenergetics **593**: 427-440, 1980.

Austin J.R., Frost E., Vidi P.-A. *et al.*: Plastoglobules are lipoprotein subcompartments of the chloroplast that are permanently coupled to thylakoid membranes and contain biosynthetic enzymes. – Plant Cell **18**: 1693-1703, 2006.

Austin J.R., Staehelin L.A.: Three-dimensional architecture of grana and stroma thylakoids of higher plants as determined by electron tomography. – Plant Physiol. **155**: 1601-1611, 2011.

Bhatti A.F., Kirilovsky D., van Amerongen H., Wientjes E.: State transitions and photosystems spatially resolved in individual cells of the cyanobacterium *Synechococcus elongatus*. – Plant Physiol. **186**: 569-580, 2021.

Canonico M., Konert G., Crepin A. *et al.*: Gradual response of cyanobacterial thylakoids to acute high-light stress – importance of carotenoid accumulation. – Cells **10**: 1916, 2021.

Canonico M., Konert G., Kaňa R.: Plasticity of cyanobacterial thylakoid microdomains under variable light conditions. – Front. Plant Sci. **11**: 586543, 2020.

Casella S., Huang F., Mason D. *et al.*: Dissecting the native architecture and dynamics of cyanobacterial photosynthetic machinery. – Mol. Plant **10**: 1434-1448, 2017.

Chenebault C., Diaz-Santos E., Kammerscheit X. *et al.*: A genetic toolbox for the new model cyanobacterium *Cyanothece* PCC 7425: A case study for the photosynthetic production of limonene. – Front. Microbiol. **11**: 586601, 2020.

Crepin A., Belgio E., Šedivá B. *et al.*: Size and fluorescence properties of algal photosynthetic antenna proteins estimated by microscopy. – Int. J. Mol. Sci. **23**: 778, 2022.

Crepin A., Cunill-Semanat E., Kuthanová Trsková E. *et al.*: Antenna protein clustering *in vitro* unveiled by fluorescence correlation spectroscopy. – Int. J. Mol. Sci. **22**: 2969, 2021.

Dekker J.P., Boekema E.J.: Supramolecular organization of thylakoid membrane proteins in green plants. – BBA-Bioenergetics **1706**: 12-39, 2005.

Engel B.D., Schaffer M., Cuellar L.K. *et al.*: Native architecture of the *Chlamydomonas* chloroplast revealed by *in situ* cryo-electron tomography. – eLife **4**: e04889, 2015.

Flannery S.E., Pastorelli F., Emrich-Mills T.Z. *et al.*: STN7 is not essential for developmental acclimation of *Arabidopsis* to light intensity. – Plant J. **114**: 1458-1474, 2023.

Flori S., Jouneau P.-H., Bailleul B. *et al.*: Plastid thylakoid architecture optimizes photosynthesis in diatoms. – Nat. Commun. **8**: 15885, 2017.

Garab G., Ughy B., de Waard P. *et al.*: Lipid polymorphism in chloroplast thylakoid membranes – as revealed by ^{31}P-NMR and time-resolved merocyanine fluorescence spectroscopy. – Sci. Rep.-UK **7**: 13343, 2017.

Gasperotti A., Brameyer S., Fabiani F., Jung K.: Phenotypic heterogeneity of microbial populations under nutrient limitation. – Curr. Opin. Biotech. **62**: 160-167, 2020.

Gu L., Grodzinski B., Han J. *et al.*: Granal thylakoid structure and function: explaining an enduring mystery of higher plants. – New Phytol. **236**: 319-329, 2022.

Gutu A., Chang F., O'Shea E.K.: Dynamical localization of a thylakoid membrane binding protein is required for acquisition of photosynthetic competency. – Mol. Microbiol. **108**: 16-31, 2018.

Gwizdala M., Botha J.L., Wilson A. *et al.*: Switching an individual phycobilisome off and on. – J. Phys. Chem. Lett. **9**: 2426-2432, 2018.

Heinz S., Rast A., Shao L. *et al.*: Thylakoid membrane architecture in *Synechocystis* depends on CurT, a homolog of the granal CURVATURE THYLAKOID1 proteins. – Plant Cell **28**: 2238-2260, 2016.

Hepworth C., Wood W.H.J., Emrich-Mills T.Z. *et al.*: Dynamic thylakoid stacking and state transitions work synergistically to avoid acceptor-side limitation of photosystem I. – Nat. Plants **7**: 87-98, 2021.

Herbstová M., Tietz S., Kinzel C. *et al.*: Architectural switch in plant photosynthetic membranes induced by light stress. – PNAS **109**: 20130-20135, 2012.

Huff J.: The Airyscan detector from ZEISS: confocal imaging with improved signal-to-noise ratio and super-resolution. – Nat. Methods **12**: i-ii, 2015.

Huokko T., Ni T., Dykes G.F. *et al.*: Probing the biogenesis pathway and dynamics of thylakoid membranes. – Nat. Commun. **12**: 3475, 2021.

Iwai M., Pack C.-G., Takenaka Y. *et al.*: Photosystem II antenna phosphorylation-dependent protein diffusion determined by fluorescence correlation spectroscopy. – Sci. Rep.-UK **3**: 2833, 2013.

Iwai M., Roth M.S., Niyogi K.K.: Subdiffraction-resolution live-cell imaging for visualizing thylakoid membranes. – Plant J. **96**: 233-243, 2018.

Iwai M., Yokono M., Kurokawa K. *et al.*: Live-cell visualization of excitation energy dynamics in chloroplast thylakoid structures. – Sci. Rep.-UK **6**: 29940, 2016.

Iwai M., Yokono M., Nakano A.: Visualizing structural dynamics of thylakoid membranes. – Sci. Rep.-UK **4**: 3768, 2014.

Jackson P.J., Hitchcock A., Brindley A.A. *et al.*: Absolute quantification of cellular levels of photosynthesis-related proteins in *Synechocystis* sp. PCC 6803. – Photosynth. Res. **155**: 219-245, 2023.

Joshua S., Mullineaux C.W.: Phycobilisome diffusion is required for light-state transitions in cyanobacteria. – Plant Physiol. **135**: 2112-2119, 2004.

Kaňa R.: Mobility of photosynthetic proteins. – Photosynth. Res.

116: 465-479, 2013.
Kaňa R., Kotabová E., Komárek O. *et al.*: The slow S to M fluorescence rise in cyanobacteria is due to a state 2 to state 1 transition. – BBA-Bioenergetics **1817**: 1237-1247, 2012.
Kaňa R., Prášil O., Komárek O. *et al.*: Spectral characteristic of fluorescence induction in a model cyanobacterium, *Synechococcus* sp. (PCC 7942). – BBA-Bioenergetics **1787**: 1170-1178, 2009.
Kaňa R., Steinbach G., Sobotka R. *et al.*: Fast diffusion of the unassembled PetC1-GFP protein in the cyanobacterial thylakoid membrane. – Life **11**: 15, 2021.
Kirchhoff H.: Diffusion of molecules and macromolecules in thylakoid membranes. – BBA-Bioenergetics **1837**: 495-502, 2014.
Kirilovsky D., Büchel C.: Evolution and function of light-harvesting antenna in oxygenic photosynthesis. – In: Grimm B. (ed.): Advances in Botanical Research. Vol. 91. Pp. 247-293. Academic Press, London 2019.
Komárek O., Felcmanová K., Šetlíková E. *et al.*: Microscopic measurements of the chlorophyll *a* fluorescence kinetics. – In: Suggett D.J., Prášil O., Borowitzka M.A. (ed.): Chlorophyll *a* Fluorescence in Aquatic Sciences: Methods and Applications. Pp. 91-101. Springer, Dordrecht 2010.
Konert G., Steinbach G., Canonico M., Kaňa R.: Protein arrangement factor: a new photosynthetic parameter characterizing the organization of thylakoid membrane proteins. – Physiol. Plantarum **166**: 264-277, 2019.
Krynická V., Skotnicová P., Jackson P.J. *et al.*: FtsH4 protease controls biogenesis of the PSII complex by dual regulation of high light-inducible proteins. – Plant Commun. **4**: 100502, 2023.
Lepetit B., Goss R., Jakob T., Wilhelm C.: Molecular dynamics of the diatom thylakoid membrane under different light conditions. – Photosynth. Res. **111**: 245-257, 2012.
Lippincott-Schwartz J., Snapp E.L., Phair R.D.: The development and enhancement of FRAP as a key tool for investigating protein dynamics. – Biophys. J. **115**: 1146-1155, 2018.
Liu L.-N., Bryan S.J., Huang F. *et al.*: Control of electron transport routes through redox-regulated redistribution of respiratory complexes. – PNAS **109**: 11431-11436, 2012.
Liu L.-N., Elmalk A.T., Aartsma T.J. *et al.*: Light-induced energetic decoupling as a mechanism for phycobilisome-related energy dissipation in red algae: a single molecule study. – PLoS ONE **3**: e3134, 2008.
MacGregor-Chatwin C., Sener M., Barnett S.F.H. *et al.*: Lateral segregation of photosystem I in cyanobacterial thylakoids. – Plant Cell **29**: 1119-1136, 2017.
Mahbub M., Hemm L., Yang Y. *et al.*: mRNA localization, reaction centre biogenesis and thylakoid membrane targeting in cyanobacteria. – Nat. Plants **6**: 1179-1191, 2020.
Malacrida L., Hedde P.N., Ranjit S. *et al.*: Visualization of barriers and obstacles to molecular diffusion in live cells by spatial pair-cross-correlation in two dimensions. – Biomed. Opt. Express **9**: 303-321, 2018.
Mareš J., Strunecký O., Bučinská L., Wiedermannová J.: Evolutionary patterns of thylakoid architecture in cyanobacteria. – Front. Microbiol. **10**: 277, 2019.
Mueller F., Mazza D., Stasevich T.J., McNally J.G.: FRAP and kinetic modeling in the analysis of nuclear protein dynamics: what do we really know? – Curr. Opin. Cell Biol. **22**: 403-411, 2010.
Mueller F., Morisaki T., Mazza D., McNally J.G.: Minimizing the impact of photoswitching of fluorescent proteins on FRAP analysis. – Biophys. J. **102**: 1656-1665, 2012.
Mullineaux C.W.: Function and evolution of grana. – Trends Plant Sci. **10**: 521-525, 2005.
Mullineaux C.W.: Factors controlling the mobility of photosynthetic proteins. – Photochem. Photobiol. **84**: 1310-1316, 2008.
Mullineaux C.W., Liu L.-N.: Membrane dynamics in phototrophic bacteria. – Annu. Rev. Microbiol. **74**: 633-654, 2020.
Mullineaux C.W., Tobin M.J., Jones G.R.: Mobility of photosynthetic complexes in thylakoid membranes. – Nature **390**: 421-424, 1997.
Mustárdy L., Garab G.: Granum revisited. A three-dimensional model – where things fall into place. – Trends Plant Sci. **8**: 117-122, 2003.
Muzzopappa F., Kirilovsky D.: Changing color for photoprotection: The orange carotenoid protein. – Trends Plant Sci. **25**: 92-104, 2020.
Pribil M., Labs M., Leister D.: Structure and dynamics of thylakoids in land plants. – J. Exp. Bot. **65**: 1955-1972, 2014.
Rast A., Schaffer M., Albert S. *et al.*: Biogenic regions of cyanobacterial thylakoids form contact sites with the plasma membrane. – Nat. Plants **5**: 436-446, 2019.
Scipioni L., Lanzanó L., Diaspro A., Gratton E.: Comprehensive correlation analysis for super-resolution dynamic fingerprinting of cellular compartments using the Zeiss Airyscan detector. – Nat. Commun. **9**: 5120, 2018.
Solymosi K.: Plastid structure, diversification and interconversions I. Algae. – Curr. Chem. Biol. **6**: 167-186, 2012.
Steinbach G., Schubert F., Kaňa R.: Cryo-imaging of photosystems and phycobilisomes in *Anabaena* sp. PCC 7120 cells. – J. Photoch. Photobio. B **152**: 395-399, 2015.
Strašková A., Knoppová J., Komenda J.: Isolation of the cyanobacterial YFP-tagged photosystem I using *GFP-Trap*®. – Photosynthetica **56**: 300-305, 2018.
Strašková A., Steinbach G., Konert G. *et al.*: Pigment-protein complexes are organized into stable microdomains in cyanobacterial thylakoids. – BBA-Bioenergetics **1860**: 148053, 2019.
Tichý M., Bečková M., Kopečná J. *et al.*: Strain of *Synechocystis* PCC 6803 with aberrant assembly of photosystem II contains tandem duplication of a large chromosomal region. – Front. Plant Sci. **7**: 648, 2016.
Verhoeven D., van Amerongen H., Wientjes E.: Single chloroplast *in folio* imaging sheds light on photosystem energy redistribution during state transitions. – Plant Physiol. **191**: 1186-1198, 2023.
Vermaas W.F.J., Timlin J.A., Jones H.D.T. *et al.*: *In vivo* hyperspectral confocal fluorescence imaging to determine pigment localization and distribution in cyanobacterial cells. – PNAS **105**: 4050-4055, 2008.
Wassie A.T., Zhao Y., Boyden E.S.: Expansion microscopy: principles and uses in biological research. – Nat. Methods **16**: 33-41, 2019.
Weiner E., Pinskey J.M., Nicastro D., Otegui M.S.: Electron microscopy for imaging organelles in plants and algae. – Plant Physiol. **188**: 713-725, 2022.
Wilhelm C., Goss R., Garab G.: The fluid-mosaic membrane theory in the context of photosynthetic membranes: Is the thylakoid membrane more like a mixed crystal or like a fluid? – J. Plant Physiol. **252**: 153246, 2020.
Williams J.G.K.: Construction of specific mutations in photosystem II photosynthetic reaction center by genetic engineering methods in *Synechocystis* 6803. – Method. Enzymol. **167**: 766-778, 1988.
Wilson A., Ajlani G., Verbavatz J.-M. *et al.*: A soluble carotenoid protein involved in phycobilisome-related energy dissipation in cyanobacteria. – Plant Cell **18**: 992-1007, 2006.
Yokoo R., Hood R.D., Savage D.F.: Live-cell imaging of

cyanobacteria. – Photosynth. Res. **126**: 33-46, 2015.
Zhang Z., Zhao L.-S., Liu L.-N.: Characterizing the supercomplex association of photosynthetic complexes in cyanobacteria. – Royal Soc. Open Sci. **8**: 202142, 2021.
Zhao L.-S., Li C.-Y., Chen X.-L. *et al.*: Native architecture and acclimation of photosynthetic membranes in a fast-growing cyanobacterium. – Plant Physiol. **190**: 1883-1895, 2022.